Water Research 286 (2025) 124213

Contents lists available at ScienceDirect

Water Research

journal homepage: www.elsevier.com/locate/watres

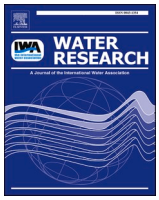

Influence of particulate matter air quality on water quality of atmospheric water harvesting

Matthew Russell [a,b], Alex Webster [c], Carl Abadam [b,d], Katelin Fisher [b], Stephanie Campbell [b,d], Carmen Atchley [b,d], Kana Radius [b,d], Paris Eisenman [b,d], Ashley Apodaca-Sparks [b,d], Astrid Gonzaga [b,d], Rui Liu [e], Patrick Hudson [f], Anjali Mulchandani [a,b,d,*]

[a] Water Resources Program, MSC05 3110, 1 University of New Mexico, Albuquerque, NM, 87131, USA
[b] Center for Water and the Environment, MSC01 1070, 1 University of New Mexico, Albuquerque, NM, 87131, USA
[c] Department of Biology, MSC03 2020, 1 University of New Mexico Albuquerque, NM, 87131, USA
[d] Department of Civil Engineering, MSC01 1070, University of New Mexico, Albuquerque, NM, 87131, USA
[e] College of Pharmacy, MSC09 5360, 1 University of New Mexico, Albuquerque, NM, 87131, USA
[f] Environmental Health Department, City of Albuquerque, 1 Civic Plaza NW, Albuquerque, NM, 87102, USA

ARTICLE INFO

Keywords:
Dehumidification
Condensation
Aerosols
Water vapor
Pollutants

ABSTRACT

Atmospheric water harvesting (AWH) is a decentralized water technology that dehumidifies air to provide water. When atmospheric water is condensed, other atmospheric particles and gases can enter the liquid water. For AWH to serve as drinking water, it is necessary to understand how these air constituents interact with water as it condenses and the resulting water quality. The objectives of this research were to determine: i) the variation of measured air and water quality contaminants at two sites, and ii) the extent of interaction between particulate matter concentration in the air and the water quality of atmospherically harvested water. This study performed AWH using compressor dehumidifiers at industrial and urban ambient air quality monitoring sites in Albuquerque, New Mexico, USA. Air contamination was greater at the industrial site compared to the urban site (range $PM_{2.5}$ urban 1.3 – 33.4 μg/m^3, industrial 1.8 – 127.5 μg/m^3; range PM_{10} urban 3.7 – 99.2 μg/m^3, industrial 4.4 – 1525 μg/m^3). Water trace metals concentrations and turbidity were also greater at the industrial site. Aluminum concentrations ranged 22.9 – 600 μg/L (urban) and 22.1 – 1560 μg/L (industrial); Iron ranged 0.5 – 363 μg/L (urban), 3.4 – 828 μg/L (industrial); Manganese ranged 0.7 – 23.7 μg/L (urban), 1.3 – 69.2 μg/L (industrial); and turbidity ranged 0.3 – 28 NTU (urban), 0.5 – 52 NTU (industrial). Water quality exceeded U.S. EPA regulations for aluminum (39 % of samples at urban site, and 90 % of samples at industrial site > 200 μg/L) and turbidity (96 % at urban site, 100 % at industrial site > 0.3 NTU). A linear mixed-effects statistical model showed water quality was a function of air quality, but for only some parameters. At the industrial site, there was a strong positive relationship between $PM_{2.5}$ and some metals (aluminum, calcium, iron [$p<0.05$]), and marginal significance with other metals (potassium, zinc [$p<0.1$]). At the urban site, there was only a strong positive relationship between $PM_{2.5}$ and calcium. Large variations in PM concentrations and site differences in their characteristics could play an important role in how much of metals in the air enters atmospherically harvested water. Findings from this study can guide research on understanding if air quality can be used to predict AWH water quality, provide insight to further understand the mechanisms of interaction between gas-phase water and particles as they move from the air to condensed water, and drive treatment decisions to meet water quality goals.

Article under review in Water Research.
* Corresponding author at: MSC01 1070 Civil Engineering, University of New Mexico, Albuquerque, NM 87131.
E-mail address: anjalim@unm.edu (A. Mulchandani).

https://doi.org/10.1016/j.watres.2025.124213
Received 25 March 2025; Received in revised form 5 July 2025; Accepted 11 July 2025
Available online 11 July 2025

1. Introduction

Global warming and the increased variability and intensity of natural disasters (e.g., floods, droughts, wildfire) are a continuing concern to water supplies. Any of these natural disasters can impact municipal water supplies and limit access for weeks to months. The atmosphere is an alternative freshwater reservoir that contains 12,900 km^3 of water (Shiklomanov, 1991), is universally accessible, and can serve as a water source when other supplies are inaccessible. Atmospheric water harvesting (AWH) can condense this available water vapor to provide access to water for communities in need during emergencies (Gayoso et al., 2024; Mulchandani and Westerhoff, 2020).

There are few studies on AWH water quality, and the relationship between air quality and water quality has only been minimally investigated for both condensation and sorption-based systems (Mulchandani et al., 2022; Zeng et al., 2024). These AWH water quality studies are often performed at a single site for around 12 months (Mulchandani et al. 2022), while few have studied AWH across multiple sites and months (Xia et al., 2015). These studies find turbidity, aluminum, iron, and manganese concentrations above United States Environmental Protection Agency (U.S. EPA) and World Health Organization (WHO) drinking water regulations in untreated AWH water, and aluminum and iron above regulatory values in treated AWH water (Zeng et al., 2024). As more studies are performed, it is apparent that there may be large variability in concentrations of metal and organic contaminants over space and time. The concentration of these contaminants may be impacted by variability in air quality, but this influence is not well studied. Xia et al. (2015) studied the relationship between particulate matter (PM) and ion contaminants in condensation-based atmospherically harvested water and found high concentrations of Cl^-, SO_4^{2-}, NH_4^+ and Ca^{2+} in industrial areas associated with soil dust and exhaust. This study was performed in a temperate climate (relative humidity ranged 60–80 %), and it is unknown whether these results are transferable or universal for all climate zones and pollution sources, specifically those experienced in more arid regions. For AWH to be considered a viable drinking water source in multiple regions, more data is needed to understand the extent and nature of air quality influence on AWH water quality. Spatial and temporal analysis across environments (e.g., arid with heavy agricultural and urban emissions sources, vs humid with heavy industrial emissions) is needed to determine the full range of potential water quality.

Air quality is influenced by natural and anthropogenic emissions of trace gases and aerosols as well as meteorological factors such as temperature, wind speed, and humidity. As such, air quality can vary across a geographic region and changes throughout the day (Hosein et al., 1977). The U.S. EPA classifies and measures outdoor air pollution by 6 criteria pollutants: ozone (O_3), carbon monoxide (CO), nitrogen dioxide (NO_2), sulfur dioxide (SO_2), lead (Pb) and particulate matter (PM) pollution (US EPA, 2015a). Of these pollutants, PM may be most likely to influence chemical makeup of AWH water quality due to the interaction between PM and gas phase water in the atmosphere.

Fig. S1 shows how PM and gas-phase water interact in the atmosphere. PM is formed through nucleation, accumulation and coarse modes. In nucleation mode, particles are freshly formed through combustion or atmospheric reactions from emissions sources such as traffic, industry and burning (EPA, 2023). These particles grow through coagulation with water vapor and other constituents to get to accumulation mode. As small particles stick together, the total particle number decreases, and the mass and surface area of each coagulated particle increase. Lastly, coarse mode generally consists of mechanically separated particles that may be resuspended from surfaces. PM is classified as fine (<2.5 μm) and coarse (<10 μm) and is often made up of clusters of different constituents depending on the emissions that influence the air quality (EPA, 2019). $PM_{2.5}$ typically contains crustal material comprising of metal compounds (Al, Cu, Fe, K, Mn, etc.), soil, small liquids, elemental carbon, volatile organic compounds and various ions (SO_4^{2-} and NO_3^-) (*Chemical Elements, Minerals, Rocks*, 2024; EPA, 2023; Hasheminassab et al., 2014). PM_{10} is typically produced by surface abrasion, sea spray, biological materials, and road, crop and livestock dust (EPA, 2023). Water vapor in the air continue to interact with particulates, which may partition with water vapor into condensed AWH waters. We theorize that when this water vapor condenses within an AWH system, particles of all sizes from various sources (e.g., traffic, industry and burning) containing constituents such as metals, carbon and gases will be collected in the harvested water and impact water quality.

Currently, there is a knowledge gap regarding the relationship between PM concentrations and characteristics, and subsequent water quality of AWH, particularly as it varies by space and time to determine site specific impacts. These relationships may vary as a function of location, climate, and air quality. Closing this gap can provide key insight on the level and type of treatment required to make AWH a viable drinking water source. If there is a significant relationship between air quality measured as PM and water quality, air could be pre-filtered to remove PM before harvesting. Alternatively, post-harvesting water treatment may be applied to remove both particles and dissolved constituents.

The objectives of this research were to determine: i) the variation of measured air and water quality contaminants by site, and ii) the extent of interaction between particulate matter concentration in the air and the water quality of atmospherically harvested water. Condensation-based AWH devices were operated in a semi-arid high-desert metropolitan city. AWH devices were co-located with air quality monitoring instrumentation to directly compare air quality with AWH water quality. The air was *not* pre-filtered, and AWH water samples were *not* filtered or treated in order to gain a full understanding of the impact of PM on water quality. We hypothesized that air pollution and AWH water pollution would be greater at the industrial site compared to the urban site. Secondly, we hypothesized that there would be a positive linear relationship between both PM_{10} and $PM_{2.5}$ and total organic carbon and metal concentrations, the nature of which may be specific to each site. Findings from this study can guide research on understanding if PM can be used to predict AWH water quality, provide insight to further understand the mechanisms of interaction between gas-phase water and particles as they move from the air to condensed water, and drive treatment decisions to meet water quality goals.

2. Methodology

2.1. Methodological overview

Atmospheric water harvesting was conducted in Albuquerque, New Mexico, USA from May through September of 2024. Two condensation-based electrical dehumidifiers were operated at two Ambient Air Monitoring Network (AAMN) sites. The following sections describe the field sites, AAMN and air quality monitoring, AWH devices, water quality measurements, and statistical analyses used to determine the extent of influence of air quality on AWH water quality.

2.2. Site description

Albuquerque-Bernalillo County is at the junction of Interstate 25 (north/south) and Interstate 40 (east/west) and experiences heavy transportation traffic across the southwestern United States. Major geographic features of the region include the Sandia Mountains to the east, the Rio Grande River flowing north-south through the center, and West Mesa lava flows and volcanic cones to the west. Elevations in the city range from 4500 ft above sea level near the river, and 6500 ft at the foothills of the mountains.

The Albuquerque-Bernalillo County Air Quality Program (AQP) is administered by the City of Albuquerque Environmental Health Department. The AQP oversees the EPA-certified Ambient Air

Monitoring Network (AAMN) stations which are located across Albuquerque-Bernalillo County for monitoring major emissions sources, regional transport and trends, and public exposure, per EPA guidance. AWH research was conducted at two of these sites, which collect data on 5 of 6 criteria air pollutants every minute and are aggregated to the hour and 24-hour periods (Lead is not measured is due to Albuquerque not having a significant source). These two sites are 9.1 miles apart and are in distinct neighborhoods and opposing quadrants of the metropolitan region.

The Del Norte High School (DN) 2ZM site, AQS 35–01–0023, is located at 4700A San Mateo Blvd NE, Albuquerque, NM 87109 [Lat: 35.134263, Long: −106.585197; elevation 5210 feet] (Fig. 1). This is an urban site located at the intersection of two arterial roads in the northeast quadrant of the county. This site will be referred to as the 'urban site.'

The South Valley (SV) 2ZV site, AQS 35–001–0029, is located at 201 Prosperity Ave SE, Albuquerque, NM 87105 [Lat: 35.0169, Long: −106.6572; elevation 4956 feet]. This is a mixed residential, industrial and agricultural site located in the Mountain View neighborhood, which is in the southwest quadrant of the county and has been identified as an environmental justice area. This site will be referred to as the 'industrial site.'

2.3. Air monitoring

The AQP operates its air monitoring network in accordance with the requirements of 40 CFR Part 58. These sites measure several parameters including meteorological data such as relative humidity (RH), precipitation, wind speed, and wind direction, gathered by various analog equipment (Climatronics, METOne, Vaisala) (City of Albuquerque: Environmental Health Department, 2022). Each site measures coarse particulate matter (PM_{10}) by Teledyne/API T640X continuous FEM, and fine particulate matter ($PM_{2.5}$) through continuous Teledyne/API T640X FEM monitors as the primary monitor, and MetOne E-FRM sequential sampler with 2.5-micron inlet cutoff to record 24-hour averages (Fig. 2**b**). (FEM = Federal Equivalence Method, FRM = Federal Reference Method) (City of Albuquerque: Environmental Health Department, 2022) (EPA, 2024a). While data is collected continuously, the AQP reports hourly averages to EPA Air Quality System, and this hourly data is what was used for this AWH study.

2.4. AWH unit

Atmospheric water harvesting was conducted using AlorAir Storm LGR Extreme electrical compressor dehumidifiers (Fig. 2). This unit was chosen because it is categorized as a low grain refrigerant (LGR) which can effectively remove water from air at lower relative humidities than conventional refrigerants, and the outer casing was for industrial applications and therefore field appropriate. The dehumidifier manufacturer specifications are as follows: refrigerant R410A, air flow 210 CFM, power requirement 115V/ 60 Hz AC, coefficient of performance 2.44 L/kWh, capacity 85 pints per day (1.68 L/h) at 60 % RH and 80°F (AHAM standard), functioning humidity range 25 – 80 %, functioning temperature range 33.8 – 104°F (*AlorAir Solutions Inc.*, 2024).

The AWH units are co-located with EPA-accredited air monitoring equipment set on a platform 10 feet off the ground on top of two metal

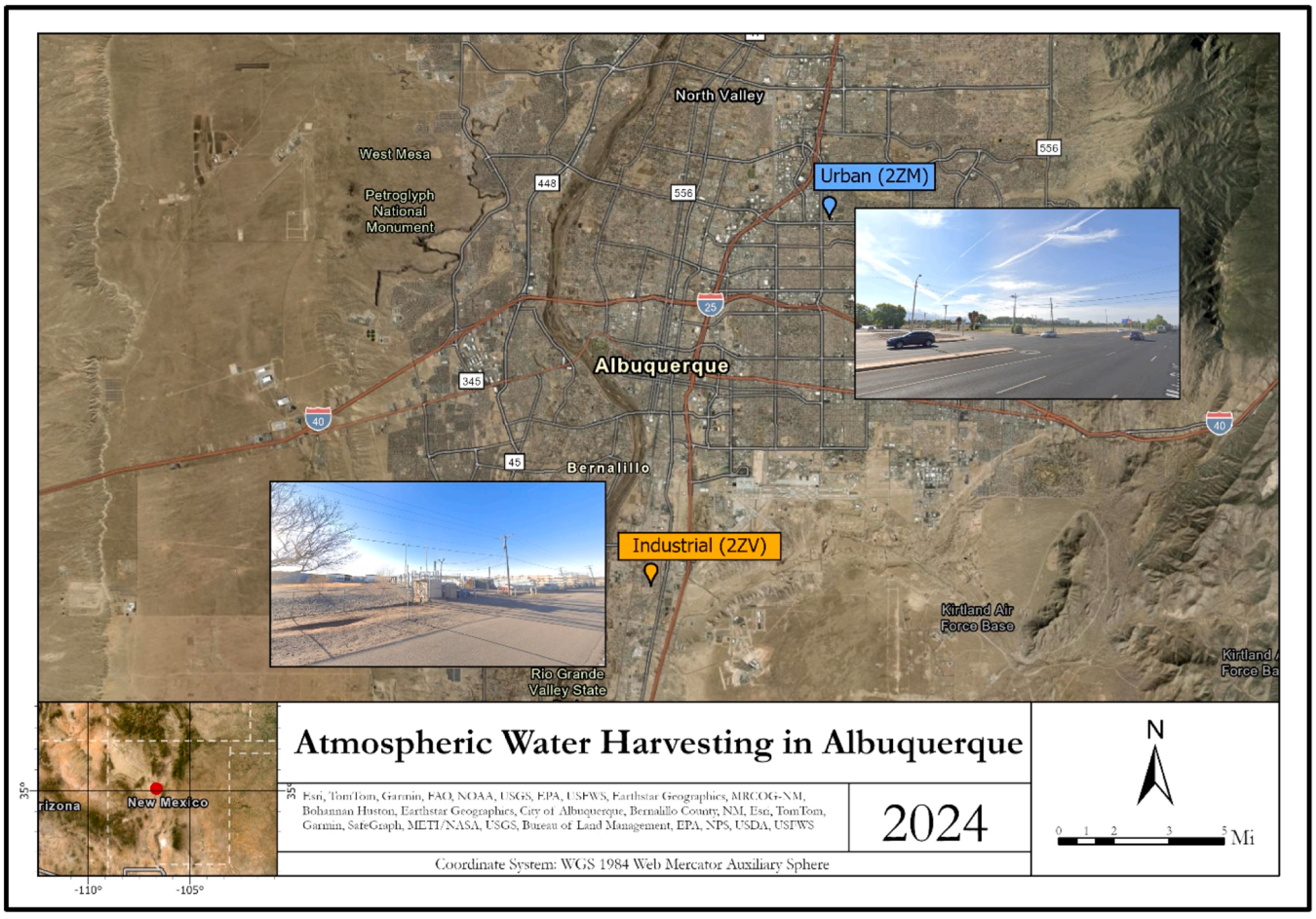

Fig. 1. Map showing locations of the two atmospheric water harvesting and air quality monitoring sites in Albuquerque, New Mexico, USA. Urban site is designated as 2ZM and industrial site as 2ZV per the City of Albuquerque Environmental Health Department Air Quality Program.

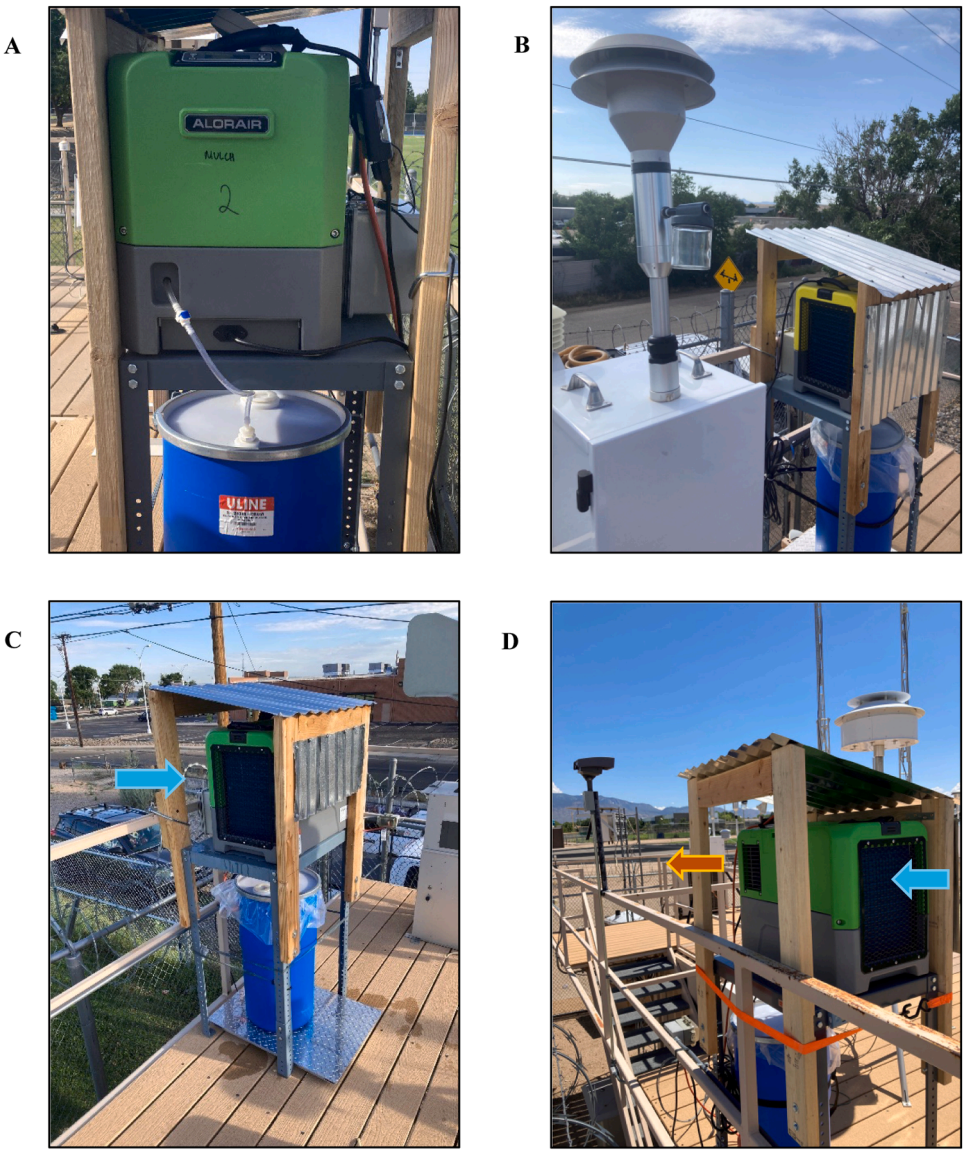

Fig. 2. (A) AWH unit at the urban site with the outlet for the water collection into the 15-gallon lined drum. (B) MetOne E-SEQ FRM for particulate matter monitoring. (C) AWH unit at the urban site. From the bottom up, Arlyn scale with 15-Gallon water collection bin sitting on top, with tubing connecting the dehumidifier to the bin. (D) Blue arrow shows air input through a large side panel into the dehumidifier, orange arrow shows dry air output.

shipping containers. A shelter structure was built to house the dehumidifier units, external water storage container, and platform scale (Fig. 2). Two AWH units were set up within 10 feet of one another. AWH units were positioned based on space availability at the air monitoring sites and to not interrupt the air monitoring instruments. At the industrial site, one AWH unit inputs (humid) air from the north and outputs (dry) air to the east. The other AWH unit is positioned with input air from the south and output to the west. At the urban site, one AWH unit inputs air from the south and outputs to the west. The other AWH unit is positioned with input air from the west and output air to the north.

A 3/8-inch-thick plastic tubing was used to directly connect water from the dehumidifier's collection reservoir to a 15-gallon drum with a new LDPE liner from HDX. The drum was placed on top of an Arlyn Scale (MKE-5), which was used to data log the weight difference before and after water harvesting.

2.5. Field methods

AWH units were operated four consecutive days per week at both field sites over two 5-hour windows of time: 8 PM to 1 AM ("Night"), and 2 AM to 7 AM ("Morning"). Historical location data for RH and PM concentrations over the past 10 years were used to determine time windows for harvesting. These time windows were chosen to collect water when relative humidity is optimal (i.e., >30 % RH) and to capture air over two different PM concentration ranges. PM concentrations are typically at their lowest during night hours, and at their peak during the morning rush hour. The 5-hour sampling window was chosen to have a long enough duration for water to be collected, while also avoiding large variation in PM concentration ranges during long collection windows. The dehumidifiers were connected to a Prime Outdoor Mechanical Timer. One unit at each site was run for the night sample while the other unit was run for the morning sample. Periodically (about every 3 weeks) the dehumidifiers designated for morning or night samples were switched to account for device variability. The total number of samples collected for the entire field campaign was 88 at the industrial site (morning = 47, night = 41) and 77 at the urban site (morning = 41, night = 36).

Every day in preparation for setup, AWH units were cleaned with 1.5-L of ultrapure (18.2 MΩ) water. A Ryobi 320 PSI power cleaner filled with ultrapure water was sprayed from the outside on the condenser

coils with even passes until 0.5-L were used. The dehumidifier purge function emptied the reservoir into a waste container. This process was performed three times (total 1.5 L), with a fourth purge to ensure all water was removed from the collection reservoir. New liners were then placed in 15-gallon drum, and a timer was set to start at 'night' or 'morning' collection times at each site.

The dehumidifiers are placed in real outdoor field conditions, and therefore some residual contamination and noise in data may be expected. To address this, a triple rinse of the coils and consecutive purging of the collection reservoir was performed to remove any residual particles that may be attached within the dehumidifier system during operation. While a blank sample of water after the 3 rinses was not collected, data over the course of the 6-month field experiment showed no consistent increase in any constituent (metals or organics). We acknowledge the assumption that the dehumidifier coils did not leach any materials into the collected water. The manual for the AlorAir Storm LGR Extreme dehumidifier states "once per year, clean the coils with an approved coil cleaner." In accordance with this advice, before deployment into the field for the first experiment, the dehumidifiers were cleaned with Purafilter 2000 Coil Cleaner, and water was flushed until TOC and metal concentrations measured below instrument detection limits.

A representative water sample was collected for lab analysis by shaking the collection bag vigorously, then using a polystyrene (PS) serological pipette to extract the sample and pipette into a nitric acid-washed 1-L Nalgene bottle. If <1-L was collected, liners were cut and drained into 1-L Nalgene. The collected water samples were stored in an insulated cooler for a maximum of two hours before either immediate analysis or preservation for future analysis. Samples preserved for total organic carbon (TOC) analysis were acidified with phosphoric acid down to pH 2, stored at 4 °C, and analyzed within 10 days. Samples preserved for trace metals analysis were acidified with high purity trace metal grade nitric acid down to pH 2, stored at 4 °C, and analyzed within one month.

2.6. Lab methods

All water quality analyses were conducted on unfiltered water samples, in order to quantify the influence of air particulate matter on water quality. The harvested water's pH, conductivity, temperature and turbidity were measured daily. The pH, conductivity and temperature were analyzed by an Oakton PC 2700 meter. Turbidity was measured using the Hach 2100Q Handheld meter, which is accurate to 0.01 NTUs. Turbidity was measured after gentle agitation of the sample to resuspend any settled particles (American Public Health Association et al., 2017). Water samples were preserved for future measurement of total organic carbon (TOC) and trace metals. TOC samples were preserved for analysis on the Teledyne Tekmar Fusion Total Organic Carbon Analyzer using UV-persulfate oxidation and non-dispersive infrared (NDIR) detector (Standard Method 5310C) (American Public Health Association et al., 2017). Trace metal samples were preserved for analysis on the Agilent 7900 Inductively Coupled Plasma Mass Spectrometer (ICP-MS). Trace metals analyzed were aluminum (Al), arsenic (As), calcium (Ca), cadmium (Cd), cobalt (Co), chromium (Cr), copper (Cu), iron (Fe), potassium (K), magnesium (Mg), manganese (Mn), sodium (Na), nickel (Ni), lead (Pb), antimony (Sb), vanadium (V), and zinc (Zn). Details for instrument detection limits are provided in the Supplemental Information (S2). Metal concentrations that were found to be below the detection limit (BDL) were given a value of half the detection limit assuming normal distribution for BDL points (Cohen and Ryan, 1989).

2.7. Statistical methods

Linear mixed-effects (LME) models in R-Studio using the 'nlme' package were used to analyze relationships between water contaminants, air concentrations and harvesting sites (Pinheiro et al., 2023; Wickham et al., 2023). Models analyzed metal or TOC concentration as a function of PM concentrations, site (urban/industrial), and their interaction, to test whether the relationship between air pollution and water quality differed across sites. The time of day was included as a random effect to account for potential variation of metal concentration during different times of day. Models aimed to test two hypotheses: i) there is a difference in metal concentrations between two sites, and ii) PM concentrations have a positive relationship with metal concentrations in collected water. The interaction term "$PM_{2.5}$ × Site" allowed the model to test if the impact was consistent across sites or varies. Model residuals were assessed for autocorrelation, normality and heteroscedasticity. Logarithmic data transformation was used to increase normality (≥0.9 for Shapiro-Wilk test) and a correlation function (AR1) was used to reduce temporal autocorrelation.

3. Results

3.1. Particulate matter air quality at each monitoring site

Table 1 shows $PM_{2.5}$ and PM_{10} concentrations at two sites: urban and industrial. $PM_{2.5}$ concentration at the urban site ranges from 1.3 to 33.4 μg/m^3, with a mean of 5.8 μg/m^3, and median of 4.4 μg/m^3. $PM_{2.5}$ at the industrial site ranges from 1.8 to 127.5 μg/m^3 and has a mean of 8.0 μg/m^3, and median of 6.4 μg/m^3. Fig. 3 shows the average PM concentration calculated over each 5-hour AWH sampling period. Using this data, the $PM_{2.5}$ concentration at the industrial site was significantly higher than at the urban site (p-value (p) <0.001, 95 % Confidence Interval (CI): 1.7 – 2.0). PM_{10} concentration at the urban site ranges from 3.7 to 99.2 μg/m^3 with mean 20.6 μg/m^3, and median of 17.5 μg/m^3; PM_{10} at the industrial site ranges 4.4 to 1525.2 μg/m^3 with mean of 47.2 μg/m^3, and median of 30 μg/m^3. The 5-hour averaged PM_{10} concentration at the industrial site was significantly higher than at the urban site ($p < 0.001$, CI: 3.3 – 3.8). The standard deviation at the industrial site was more than six times the standard deviation at the urban site (Table 1). Additional details about particulate matter concentrations over time are shown in **Fig. S2** and **Fig. S3**.

These results indicate site differences in air quality in terms of concentration for PM_x (PM_{10} and $PM_{2.5}$). The mean concentrations of PM_x for both sites fall within the "Good" category for the air quality index (AQI) (EPA, 2024b). While PM_x concentration data is available, chemical speciation data was not available at the time of this analysis. However, previous reports indicate the composition of $PM_{2.5}$ in Albuquerque, NM, is a mixture of organic carbon, nitrates, sulfates, crustal and elemental carbon (EPA, 2023).

3.2. AWH water quality at each monitoring site

A summary of water quality characteristics collected from AWH units at the two sites (urban site and industrial site) is shown in Table 1. A total of 88 samples were collected from the industrial site, and 77 samples were collected at the urban site. For descriptive statistics of water quality, we did not distinguish between the 'morning' and 'night' samples, so all data from a single site was considered together. Water collected from the urban site had pH 6.2 – 8.3, and water collected from the industrial site had pH 6.0 – 7.8 (Table 1). This pH range is similar to tap waters, which have pH 6.5 –8.0 (US EPA, 2015b). The conductivity at the urban site ranged from 7.3 – 81.2 μS/cm, and at the industrial site ranged from 13.0 – 210.1 μS/cm (Table 1). While the industrial site had higher conductivity than the urban site, conductivity remained below the U.S. EPA secondary standard for conductivity of 500 mg/L of total dissolved solids, which is equivalent to <780 μS/cm. Conductivity was higher than distilled water (0.05 μS/cm) and indicates presence of charged ion species in the water.

Turbidity at the industrial site was significantly higher than that at the urban site (Fig. 4; $p = 0.007$, 95 % CI: 2.1 – 4.3). Turbidity at the urban site ranged 0.3 - 28.1 NTU (average 2.39 NTU), while the

Table 1
Air quality and water quality parameters measured at each site (urban site and industrial site).

		Urban Site				Industrial Site				Site Difference [c]	MCL [d]
Measurement [a]	Units	Average ± SD [b]	Median [b]	Min	Max	Average ± SD [b]	Median [b]	Min	Max		
$PM_{2.5}$	μg/m³	5.8 ± 4.1	4.4	1.3	33.4	8.0 ± 7.0	6.4	1.8	127.5	B	35 [A]
PM_{10}	μg/m³	20.6 ± 12.9	17.5	3.7	99.2	47.2 ± 79.0	30	4.4	1525	B	150 [B]
Al	μg/L	166 ± 127	138	22.9	600	360 ± 213	313	22.1	1560	B	< 200**
Ca	μg/L	1373 ± 1304	932	119	7411	3697 ± 4608	1982	294	25,830	B	–
Fe	μg/L	30.8 ± 49.0	16.6	0.5	363	81.3 ± 120	40.7	3.4	828	A	< 300**
		4 % BDL	4 % BDL			2 % BDL	2 % BDL				
K	μg/L	565 ± 398	505	102	1737	1469 ± 630	1357	293	3439	B	–
Mn	μg/L	5.0 ± 4.4	3.5	0.69	23.7	11.9 ± 12.7	7.0	1.3	69.2	B	< 50**
Zn	μg/L	33.9 ± 35.6	23.9	4.0	199	37.6 ± 38.7	27.5	1.8	236	A	< 5000**
As	μg/L	0.07 ± 0.05	0.05	BDL	0.25	0.09 ± 0.09	0.05	BDL	0.50	–	< 10*
		32 % BDL	32 % BDL			18 % BDL	18 % BDL				
Cd	μg/L	0.02 ± 0.006	0.02	BDL	0.03	0.04 ± 0.04	0.03	BDL	0.28	–	< 5*
		54 % BDL	54 % BDL			17 % BDL	17 % BDL				
Co	μg/L	0.07 ± 0.18	0.04	BDL	1.37	0.11 ± 0.14	0.05	0.01	0.74	–	–
		22 % BDL	22 % BDL			10 % BDL	10 % BDL				
Cr	μg/L	0.45 ± 1.24	0.16	0.01	10.3	0.69 ± 3.0	0.21	0.02	27.3	–	< 100*
		5 % BDL	5 % BDL								
Cu	μg/L	3.5 ± 3.63	2.2	0.44	19.3	4.7 ± 5.3	2.3	0.36	27.1	–	< 1300*
Mg	μg/L	74.9 ± 83.3	45.2	2.3	489	132 ± 149	66.4	6.9	721	–	–
Na	μg/L	129 ± 160	76.8	10.3	1035	183 ± 241	85.8	BDL	1021	–	–
		15 % BDL	15 % BDL			10 % BDL	10 % BDL				
Ni	μg/L	1.85 ± 8.50	0.20	BDL	49.1	0.89 ± 3.05	0.22	BDL	19.0	–	–
		56 % BDL	56 % BDL			56 % BDL	56 % BDL				
Sb	μg/L	0.13 ± 0.15	0.08	BDL	0.75	0.21 ± 0.25	0.13	BDL	1.41	–	< 6*
		12 % BDL	12 % BDL			6 % BDL	6 % BDL				
Pb	μg/L	0.19 ± 0.35	0.09	BDL	2.25	1.23 ± 2.01	0.5	0.04	10.9	–	< 15*
		6 % BDL	6 % BDL								
V	μg/L	0.20 ± 0.18	0.16	0.02	0.93	0.34 ± 0.38	0.24	0.02	2.18	–	–
		12 % BDL	12 % BDL			4 % BDL	4 % BDL				
Conductivity	μS/cm	25.2 ± 14.4	22.5	7.3	81.2	42.5 ± 30.9	33.8	13.0	210.1	B	–
pH	–	6.9 ± 0.4	6.8	6.2	8.3	6.7 ± 0.439	6.7	6.0	7.8	A	6.5 - 8.5**
TOC	mg/L	3.9 ± 2.6	3.2	0.9	15.0	6.1 ± 6.6	4.0	0.92	39.2	A	–
Turbidity	NTU	2.4 ± 4.42	1.4	0.3	28.1	5.3 ± 9.1	2.4	0.5	52.0	B	<0.3*

[a] Total number of water samples collected was 88 at the industrial site and 77 at the urban site.
[b] BDL stands for below detection limit. If a contaminant measured any value BDL, then a percentage is shown on how many data points were BDL and only the measurements above detection limit were used to calculate for Average ± SD and median.
[c] Site differences between the average values of each parameter were calculated by the LME model. "A" indicates "no site difference," i.e. $p > 0.05$, and "B" indicates difference in average value between the urban and industrial sites ($p < 0.05$).
[d] "A" 24-hour $PM_{2.5}$ EPA primary standard and "B"24-hour PM_{10} EPA primary standard. MCL stands for Maximum Contaminant Level with "*" representing U.S. EPA primary drinking water regulations and "**" representing U.S. EPA secondary drinking water standards.

turbidity at the industrial site ranged 0.5 – 52.0 NTU (average 5.3 NTU). Turbidity indicates the presence of particles that refract light in waters (American Public Health Association et al., 2017). Higher turbidity at the industrial site may indicate dust, debris or pollen (Hasheminassab et al., 2014). The majority of the samples at both sites (96 % at the urban site, 100 % at the industrial site) had turbidity in excess of the U.S. EPA Primary Drinking Water Standard of 0.3 NTU.

Similar to turbidity, the total organic carbon (TOC) concentration at the industrial site was almost double that at the urban site (Table 1), though high variability in the data likely reduced the statistical significance of the site difference ($p = 0.18$, CI: 4.1 – 6.3). TOC at the urban site ranged 0.9 – 15.0 mg/L (average 3.9 mg/L), while TOC at the industrial site ranged 0.92 – 39.2 mg/L (average 6.1 mg/L) (Fig. 4). Likely, the constituents of TOC can include carboxylic acids and aldehydes. Aldehydes such as acetaldehyde and formaldehyde have been measured in other AWH waters, and are classified as Group 1 carcinogens by the International Agency for Research on Cancer (Mulchandani et al., 2022; O'Brien et al., 2005; Zeng et al., 2024). Sources of TOC can be both anthropogenic from vehicle and industrial emissions, and biogenic from vegetative sources (Formenti et al., 2003). In municipal drinking waters, TOC is monitored but not regulated, as it can react with disinfectants such as chlorine, or other halogens such as bromide and iodide, to form chlorinated, brominated, and iodinated disinfection byproducts (Richardson and Postigo, 2012).

Seventeen metals were monitored in all water samples, and 6 metals were detected in all samples: Al, Ca, Fe, K, Mn, and Zn. Table 1 shows the metal concentration ranges for all metals across the sites. The remaining metals (As, Cd, Co, Cr, Cu, Mg, Na, Ni, Sb, Pb, V) had several samples measured below the detection limit (BDL) of the ICP-MS instrument and/or were measured at concentrations far below water quality regulations.

Table 2 shows the LME model resulted in significant difference ($p < 0.05$) in trace metal concentration between the industrial and urban sites for Al, Ca, K, and Mn, and marginal significant difference ($p = 0.07$) for Fe. Al and Fe concentrations were 2x higher at the industrial site than at the urban site; Ca and K concentrations were almost 3x higher at the industrial site. Al concentration range at the urban site was 22.9 – 600 μg/L and at the industrial site was 22.1 – 1560 μg/L. 39 % of the samples at the urban site, and 90 % of samples at the industrial site exceed the U. S. EPA secondary maximum contaminant level (MCL) for aluminum of 200 μg/L. Fe concentration range at the urban site was 0.5 – 363 μg/L, while at the industrial site Fe ranged 3.4 – 828 μg/L. The industrial site had 3 values that exceeded the EPA secondary MCL for Fe (300 μg/L), while the urban site only had 1 exceedance. Mn concentrations only exceeded EPA secondary MCL of 50 μg/L at the industrial site, where Mn range was 1.3 – 69.2 μg/L, while at the urban site the Mn concentration was less than half of the MCL. Aluminum, iron and manganese are often characteristic of soil and dust, particularly from PM with a high fraction of crustal components and industrial sources (Hasheminassab et al., 2014). The industrial site in Albuquerque, NM is located on a dirt road near building and vehicular material industries, while the urban site is on a major paved roadway. Dust and dirt may contribute to the higher

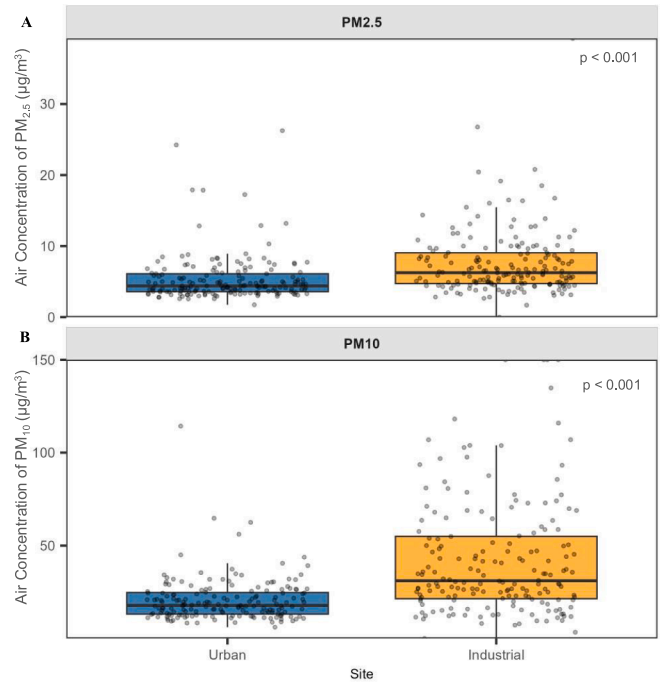

Fig. 3. $PM_{2.5}$ and PM_{10} average concentrations (µg/m^3) calculated over each 5-hour AWH sampling period. The urban site is shown as a blue box-and-whisker plot, while the industrial site is shown in orange. One data point lies outside the axes of the plot due to scale: 421.2 µg/m^3 for PM_{10} at the industrial site. Outliers are points greater than (Q3+1.5(Q3-Q1)) and less than (Q1 −1.5(Q3-Q1)), where Q is quartile. P-value is calculated from the LME model and represents significance of difference in concentrations of PM between the two sites.

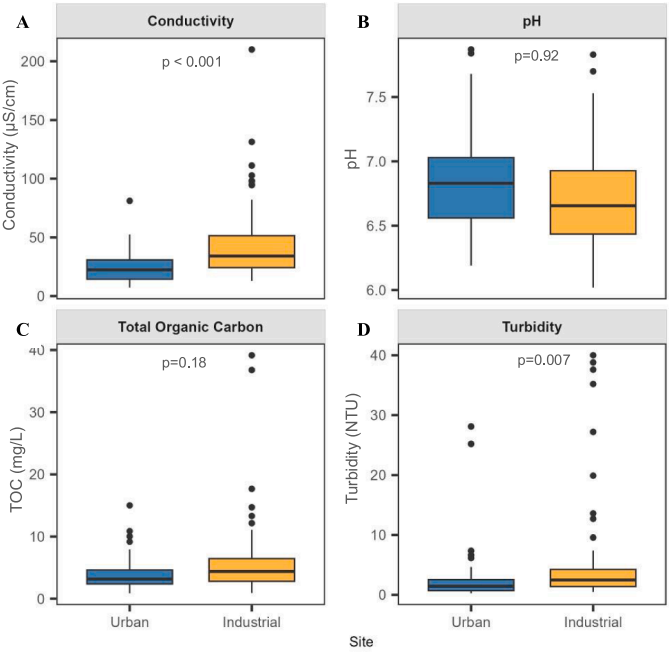

Fig. 4. Water quality characteristics for two sites, urban site – blue, and industrial site – orange. Conductivity (A), pH (B), total organic carbon (TOC) (C) and turbidity (D). Outliers are points greater than (Q3+1.5(Q3-Q1)) and less than (Q1 −1.5(Q3-Q1)), where Q is quartile. One turbidity data point (52.0 NTU at the industrial site) is not shown because it lies outside the axes of the plot due to scale.

Table 2
LME model outputs for site differences in metal concentrations at the industrial site compared to the urban site.

Metal Concentration (µg/L)	LME Model Output of Site Differences		
	Intercept	CI Range	p-value[a]
Al	247	81: 412	0.04*
Ca	963	675: 1160	<0.001***
Fe	16.2	8.9: 29.5	0.07
K	1220	610: 1840	<0.001***
Mn	5.6	4.3: 7.3	<0.001***
Zn	24.4	16.2: 38.2	0.94

[a] p-values: * <0.05, ** <0.01, *** <0.001.

concentration of these crustal metals in the industrial site samples.

Ca and K showed strong significant difference between the urban and industrial site (Ca $p < 0.001$, CI: 675 – 1160; K $p < 0.001$, CI: 610 – 1840). These confidence intervals indicate that there is a strong difference in metal concentration between the two sites, but there is also a large variability possibly due to the large variability in air quality, particularly at the industrial site. Atmospheric dust may contain calcium in the form of calcium carbonate (EPA, 2019), while potassium is associated with $PM_{2.5}$, rainwater and biomass burning (EPA, 2019; Hasheminassab et al., 2014). While both elements are not considered health hazards, Ca is characteristic of water hardness. At the Ca concentrations measured in this study (≤ 25 ppm), this water would be considered very soft.

3.3. Particulate matter relationship with water quality

Table 3 and Fig. 5 shows concentrations of Al, Fe, and Ca significantly increase as $PM_{2.5}$ increases at the industrial site, indicating a positive relationship between $PM_{2.5}$ and these metals (Al, Ca, Fe) at the industrial site. Ca exhibited the highest significance ($p = 0.009$, slope 1.98 $\mu g_{Ca}\, L^{-1} \mu g_{PM_{2.5}}^{-1} m^3$); Al showed the highest positive slope at 16.3 $\mu g_{Al}\, L^{-1} \mu g_{PM_{2.5}}^{-1} m^3$, $p = 0.02$; Fe had similar slope to Ca, 2.1 $\mu g_{Fe}\, L^{-1} \mu g_{PM_{2.5}}^{-1} m^3$, $p = 0.05$. The slope value indicates the unit increase in metal concentration (µg $_L^{-1}$) for every unit increase in PM (µg m^{-3}). For example, Al concentration will increase by 16 µg $_L^{-1}$ for every µg m^{-3} unit increase in $PM_{2.5}$, while Fe and Ca unit concentrations will increase by 2 µg $_L^{-1}$ for every µg m^{-3} unit increase in $PM_{2.5}$. $PM_{2.5}$ in the Albuquerque, NM region has been characterized to have a large fraction of crustal components and organic carbon (EPA, 2023). These crustal components may be more present at this specific industrial site due to its landscape, including dirt roads and unconsolidated soil or bare soil. These trends could apply in other industrial regions, where $PM_{2.5}$ can contain crustal (i.e., metal) sources from dust and resuspended soil, and mineral sources from vehicle emissions and industrial emissions (e.g., metallurgical, petrochemical, phosphate) (Alastuey et al., 2006; Upadhyay et al., 2011).

Additional metals that could be associated with $PM_{2.5}$ include Mn, Zn, and K. Mn is characteristic of dust, K is characteristic of $PM_{2.5}$ and biogenic burning, and Zn is industrial and vehicular emissions, and all elements have been characterized in $PM_{2.5}$ in other regions (Hasheminassab et al., 2014). There was a non-significant pattern of an apparent relationship ($p < 0.10$) between concentrations of K ($p = 0.10$) and Mn ($p = 0.07$) in AWH waters and $PM_{2.5}$ at the industrial site in this study (Table 3 and Fig. 5).

Meanwhile, there were no statistical relationships found between AWH metals concentrations and PM_{10}, except for Ca (Table 3 and Fig. 6). Water vapor is likely to associate with small particles (~100 nm) during the accumulation mode of heterogeneous nucleation (**Fig. S1**). Smaller $PM_{2.5}$ (i.e. <2.5 μm) is more likely to partition from air to water when water vapor condenses, while the larger PM_{10} may not travel alongside the condensed water and collect in the harvesting basin.

Table 3
LME model outputs for metal concentrations and PM_x relationship with site as fixed effect.

Metal Concentration (μg/L)	Urban site $PM_{2.5}$ and Metal Relationship [a,c]			Industrial site $PM_{2.5}$ and Metal Relationship			Urban site PM_{10} and Metal Relationship			Industrial site PM_{10} and Metal Relationship		
	Slope	CI Range	p-value[b]	Slope	CI Range	p-value[b]	Slope	CI Range	p-value[b]	Slope	CI Range	p-value[b]
Al	3.7	−4.9: 12.2	0.40	16.3	−3.2: 35.7	0.02*	0.4	−2.9: 3.8	0.27	2.3	−4.4: 9.1	0.79
Ca	1.0	1.00: 1.04	0.03*	1.98	1.95: 2.02	0.009**	1.0	1.00: 1.02	0.01**	2.0	1.98: 1.01	0.04*
Fe	2.0	0.92: 1.04	0.42	2.1	1.92: 2.20	0.049*	1.0	0.98: 1.03	0.76	2.0	1.96: 2.06	0.67
K	9.3	−17.8: 36.4	0.50	39	−23.8: 102	0.10	4.8	−6.2: 15.8	0.38	5.1	−17.1: 27.3	0.95
Mn	1.0	0.97: 1.02	0.80	2.0	1.95: 2.06	0.35	1.0	0.99: 1.01	0.65	1.0	1.98: 2.02	0.71
Zn	1.0	0.93: 1.02	0.23	2.1	1.93: 2.13	0.07	1.0	0.98: 1.02	0.92	1.0	1.97: 2.04	0.66

[a] For each column, the rows represent 95 % confidence intervals (CI) for minimum and maximum confidence and p-value. "Site PM_x and Metal Relationship" looks at the relationship between PM_x ($PM2_{2.5}$ and PM_{10}) and site (urban or industrial).
[b] p-values: * <0.05, ** <0.01, *** <0.001.
[c] R^2 for LME model reported in Supplemental Information S4, Table S2 and Table S3.

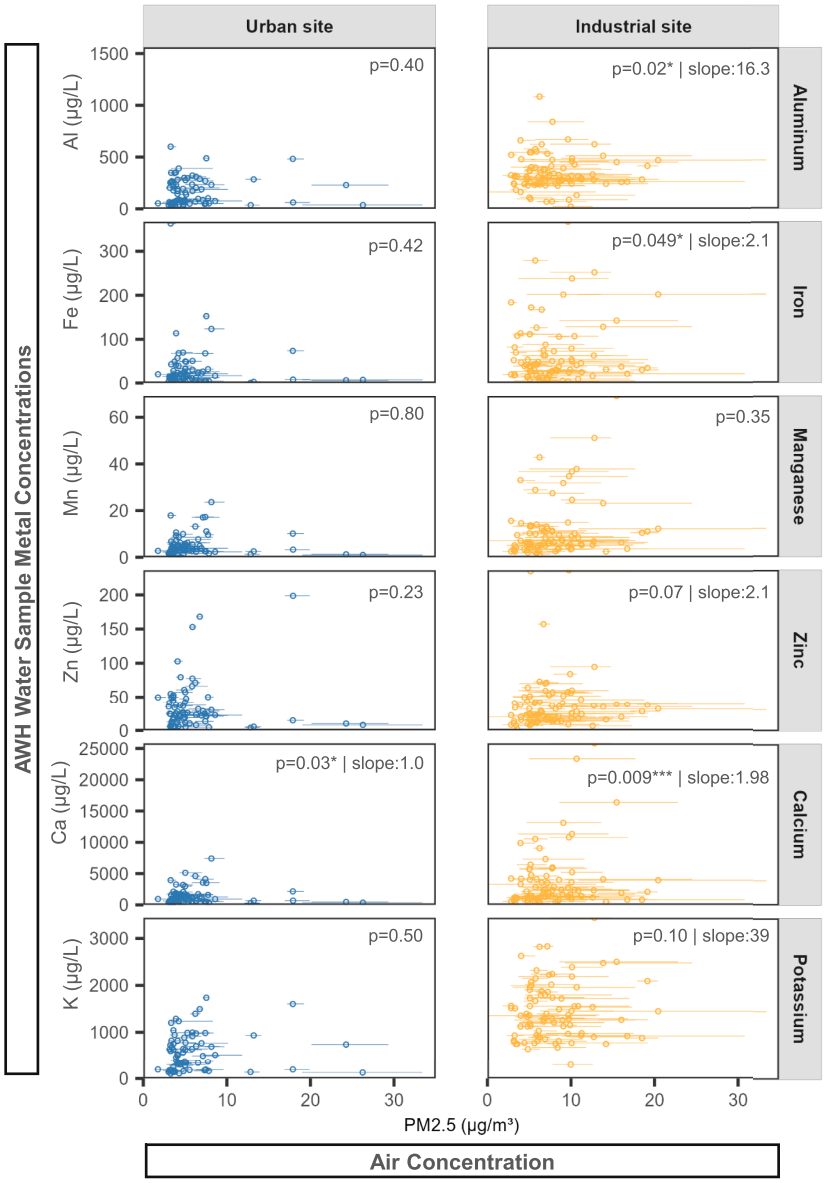

Fig. 5. $PM_{2.5}$ concentrations and the relationship to 5 metals (Al, Ca, Fe, K, Mn). The open dot represents the average $PM_{2.5}$ concentration with the horizontal bars representing the minimum and maximum concentrations during the 5-hr collection window. Some values were excluded from the graphs due to axes limits and clarity: i) One $PM_{2.5}$ value at the industrial site has an average of 39.2, min:4.4, max:127.5 μg/m³. The corresponding concentration of metals are 1560.4 μg Al/L, 828.4 μg Fe/L, 53.3 μg Mn/L, 41.3 μg Zn/L, 12,201.4 μg Ca/L, 3282.0 μg Ca/L. ii) industrial site, $PM_{2.5}$ average 6.23, min: 5.5, max:6.9 μg/m³ and Fe 562.493 μg/L; iii) industrial site $PM_{2.5}$ average 10.3, min: 7.0, max:14.8 μg/m³, 5232.1 μg K/L. P-values: * <0.05, ** <0.01, *** <0.001.

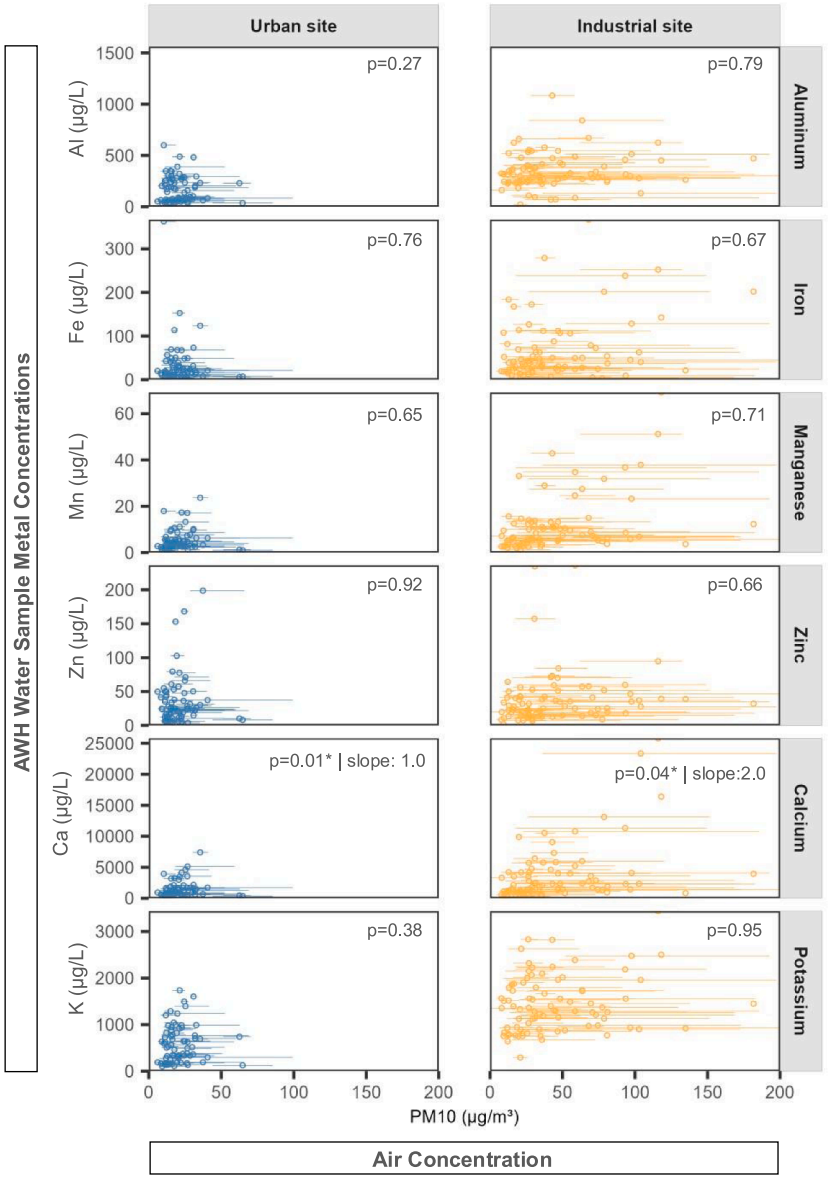

Fig. 6. PM_{10} concentrations and the relationship to 5 metals (Al, Ca, Fe, K, Mn). The dot represents the average PM_{10} concentration with the bars representing the minimum and maximum concentrations during that collections window. One industrial PM_{10} point at 134 $\mu g/m^3$has max outside the bounds of the axes (min 30.8, max 338.5 $\mu g/m^3$). Some values were excluded from the graphs due to axes limits and clarity: i) industrial site, PM_{10} average 421.2, min:33.7, max:1525.2 $\mu g/m^3$, 1560.4 µg Al/L, 828.4 µg Fe/L, 53.3 µg Mn/L, 41.3 µg Zn/L, 12,201.4 µg Ca/L, 3282.0 µg K/L; ii) industrial site, PM_{10} average 42.9, min: 28.2, max:58.5 $\mu g/m^3$ and Fe concentration 562.5 µg/L; iii) industrial site, PM_{10} average 90.7, min: 56.0, max: 146.3 $\mu g/m^3$ and K concentration of 5232.1 µg/L. P-values: * <0.05, ** <0.01, *** <0.001.

3.4. Potential influences of AWH collection volume on water quality

Water quality, measured as concentration of a constituent, may be influenced by the volume of water harvested during any given sample period. **Fig. S4** shows the volume of water harvested during each sample collection varied with relative humidity. While all samples were collected over a 5-hour period, water volume ranged from 0 – 8.6 L. Fig. 7 shows a dilution effect for Ca, Fe, Al, conductivity, TOC and turbidity. For example, when water volume was low (1 L collected over 5 h), Fe concentration was 3x – 4x higher than when volume was in the 2.5 – 8.6 L range. Similarly, when the water volume was <2 L collected over 5 h, turbidity reached as high as 40 NTU but remained below 10 NTU for larger water volumes (>2.5 L over 5 h). These results indicate that larger collection volumes can dilute the mass of air contaminants and lead to a lower measured concentration, while small water volumes amplify the mass when represented as concentration. A breakpoint analysis could be performed to identify the specific inflection point where concentrations of these water constituents become more diluted and the relationship between the concentration of a constituent and the water volume changes (Piao et al., 2023). The inflection point was not calculated for this study. A visual inspection of the graphs shows the breakpoint possibly occurs between 2 – 2.5 L of water collected over 5 h for constituents such as turbidity and iron. However, for TOC and conductivity, the inflection is near 1 L of water harvested over 5 h. It is likely that the inflection point could vary based on the size of the AWH instrument as well as characteristics of specific constituents. This dilution effect should be further studied to more fully understand air quality composition and contaminant mass impacts on water quality.

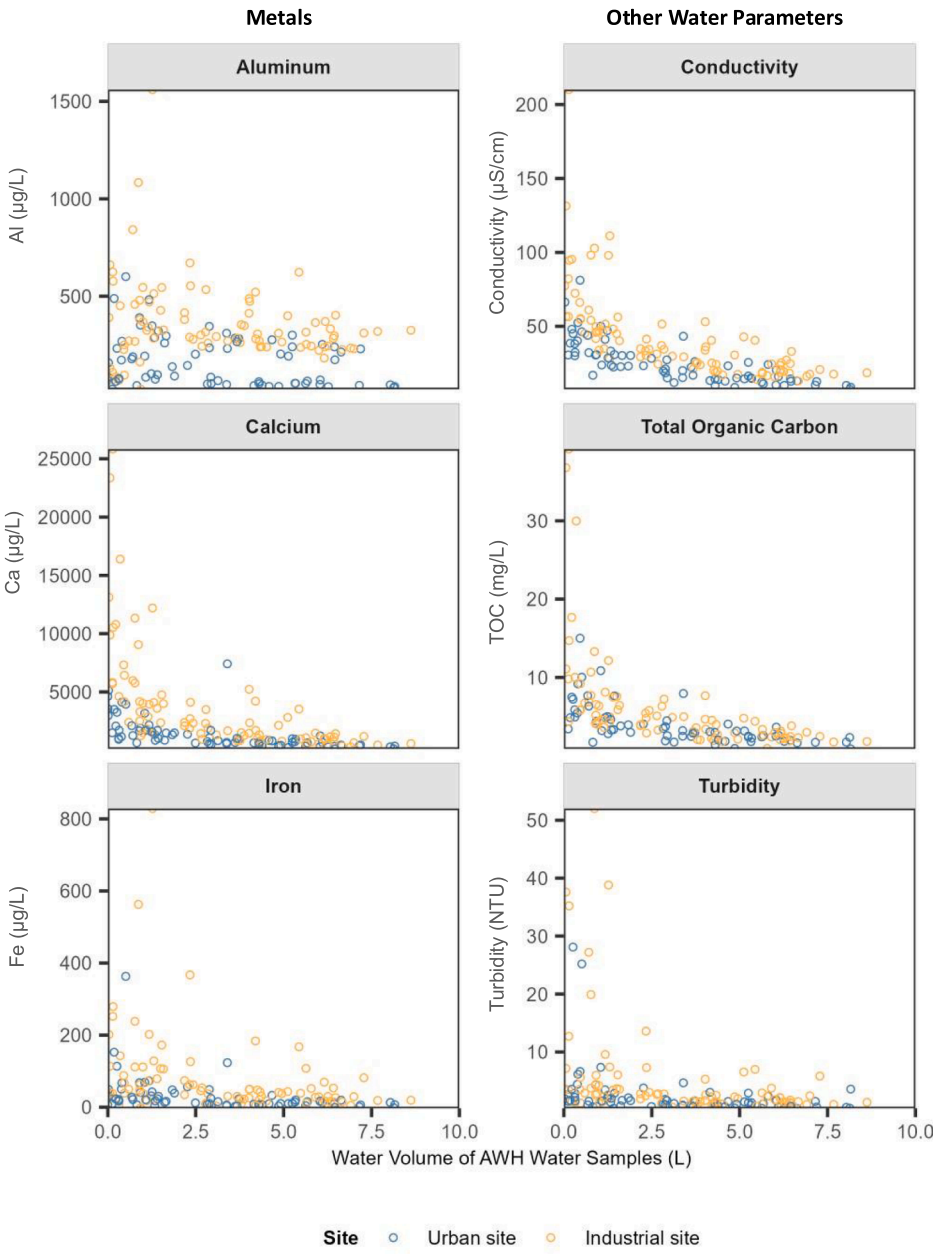

Fig. 7. The water volume collected over 5-hours and the relationship with water quality measurements with each site in a distinct color, urban site in blue and the industrial site in orange. The first column shows 3 metals, and the second column shows other water quality parameters.

4. Discussion

4.1. Atmospheric water harvesting general water quality considerations

AWH may potentially be utilized as a drinking water supply in emergency scenarios. Therefore, understanding what contaminants could be in the water in a range of scenarios is imperative. In this study, water quality was characterized as pH, conductivity, turbidity, total organic carbon, and trace metals. Ions (e.g., NO_3^-, SO_4^{2-}), volatile organic compounds (VOCs) and microbial constituents (e.g., heterotrophic plate count, opportunistic pathogens) were not considered for this study, but these may all be present in the waters (Crank, 2025; Jahne et al., 2018, 2023; 2024; Xia et al., 2015; Zeng et al., 2024). TOC concentrations measured in this study align with those measured in two other AWH studies. Mulchandani et al. (2022) tested both desiccant and condensation-based AWH systems outdoors and measured TOC between 0.5 – 14 mg/L, while (Zeng et al., 2024) tested sorption desiccant-based AWH systems indoors and measured dissolved organic carbon (DOC) between 15.4 – 52.5 mg/L. This condensation-based study showed a range of TOC values between both sites from 0.9 – 39.2 mg/L. The high variability of TOC values for each study is worth noting and should be examined further for water treatment considerations. Several metals were above U.S. EPA MCL levels and cause for concern. The aluminum concentration for EPA Secondary MCL is 200 µg/L, and both Mulchandani et al. (2022)'s condensation and desiccant-based study and this condensation-based study measured Al values above that concentration. The same trend is observed for turbidity, with prior work on both condensation and desiccant systems (Mulchandani et al., 2022; Zeng et al., 2024) and this study having values above the EPA MCL of 0.3 NTU. Multiple instances of water contaminants above regulations signify some level of water treatment is needed. Additionally, the variability of concentrations indicates the samples could be more or less contaminated depending on the collection location or time window, and level of treatment would then need to correspond.

Knowing the type and concentration of contaminants in AWH water can better inform on what water treatment will be needed to remove those contaminants and make it safe to drink. Trace metals may be removed by adsorption or filtration, and the extent of treatment would vary by site based on the extent of contamination. While this study did not pre-filter the air, this treatment could also be implemented to reduce contaminants associated with PM prior to them partitioning into condensed water.

Further, this study revealed an inverse relationship between harvested water volume and water quality. This concentration/dilution effect had a breakpoint at around 1 – 2 L of water harvested over 5 h. It is likely that this breakpoint will vary as a function of device size, air flow rate, and harvesting time (i.e., 1 hr. vs 5 hrs.). If water were harvested over longer periods of time, concentrations of contaminants may be further diluted to a baseline that can be used to design appropriate water treatment.

4.2. Air pollution sources and site-dependent factors influence atmospheric water harvesting water quality

Both $PM_{2.5}$ and PM_{10} showed a wider range of concentration at the industrial site ($PM_{2.5}$: 1.8 – 127.5 μg/m^3, PM_{10}: 4.4 – 1525 μg/m^3), which could have some potential impacts on PM_x associated metals partitioning into atmospherically harvested waters. Specifically, the variability of the $PM_{2.5}$ air quality may relate to the variability of metal contaminant concentrations. This variability may contribute to why stronger relationships were found at the industrial site, but not at the urban site. Our results demonstrate a positive relationship between $PM_{2.5}$ and aluminum, calcium and iron at the industrial site, but there was a wide range in strength of this relationship (Table 3). Large variations in PM concentrations could play an important role in how much of metals in the air coming from crustal material enters atmospherically harvested water, particularly in the Southwest United States where this study was conducted.

The industrial and urban sites showed significant differences in water quality, measured as turbidity, total organic carbon, and trace metals concentrations. AWH water quality differences by site could be due to the different sources of $PM_{2.5}$ in the urban and industrial regions. Water contamination in an industrial setting was higher than an urban setting, particularly for aluminum, manganese and turbidity, and water quality often exceeded U.S. EPA Drinking Water MCLs for several trace metals and turbidity at both sites. Our results suggest that site factors may play a large role in the level of contamination of waters at each site. For example, the industrial site had a higher contribution from dust and nearby industrial activities, while the urban site was only impacted by roadway traffic. These interactions need to be investigated as some water contaminants varied in concentration or contained values above regulations. Broadly, $PM_{2.5}$ can come from vehicular emissions, soil, biomass burning, and mixed industrial and road dust (Alastuey et al., 2006; Hasheminassab et al., 2014; Upadhyay et al., 2011). The industrial air quality monitoring site contained more open space and landscape and could therefore have more soil characteristics influencing $PM_{2.5}$. These site-based differences in the air quality of $PM_{2.5}$ appear to influence the water quality of AWH. Hasheminassab et al. (2014) discovered $PM_{2.5}$ with soil sources contained more aluminum, calcium, and iron; these same metals were found to have stronger relationships with PM and AWH statistical analysis in this study. Meanwhile, vehicular emissions and road dust sources typically show iron, calcium, manganese and zinc. Yet, the urban site water quality measurements for aluminum, iron, potassium, manganese or zinc did not show a relationship with $PM_{2.5}$.

These results indicate a need for higher resolution spatial sampling and data for both air quality and AWH water quality. Particulate matter air quality and AWH water quality showed significant site-based differences across two locations in Albuquerque, NM that were just under ten miles apart. The resolution of data matters in accurately knowing site specific characteristics, which can vary over only a few miles. The U. S. EPA reports that in New Mexico, and across the Southwestern United States, $PM_{2.5}$ is typically composed of high amounts of crustal material and organic carbon. While on average this could be correct, allocating broad resolution may be useful for general trends over very large spatial areas, but could be a limitation for investigating unique areas within a region. Studies moving forward with air quality or AWH water quality should consider gathering data from several locations in a city to capture nuances in spatial variability. This study also indicates a need for future research on the characteristics of PM_x. These studies can be bi-directional: AWH water quality studies can inform on localized aerosol composition, while aerosol composition studies can better help predict resulting condensed AWH water quality.

4.3. Broader impacts of study findings on AWH for emergency water use

Natural disasters are predicted to increase in terms of both frequency and intensity (Banholzer et al., 2014). Disasters such as fires and flooding cause devastating impacts on community infrastructure, and municipal water supply can be particularly vulnerable (Ramsayer, 2021; Robinne et al., 2021). AWH can be deployed as a decentralized water source that aids in the relief effort. However, this study highlights the importance of site selection, as we found that air quality and location significantly influence AWH water quality. From an air quality and human health perspective, high concentration of PM_x can be detrimental to human health but its composition can also increase in toxicity depending on where and what the source is (Schneider and Abbatt, 2022; Wang et al., 2023). Sources such as wildfires can increase the toxicity of airborne particles and further harm people's respiratory systems (Schneider and Abbatt, 2022). If AWH were to be utilized in high air pollution zones or as post-wildfire water relief, a better understanding of the sources and characteristics of PM could better inform communities of the extent of PM interaction and water quality contamination of AWH waters during these use case scenarios. As this study found, the location of the AWH within the city could result in varying water qualities, especially areas with high industrial activity. Thus, understanding air quality variations, the developing relationships between aerosol composition and AWH water quality, and determining optimal locations for AWH deployment is crucial for ensuring better water quality and determining appropriate treatment needs.

5. Future outlook on influences of air quality and site characteristics on AWH water quality

This study's findings show the importance of analyzing data from the two sites separately as fixed effects, as different trends were found at each site. If the urban site was the only site analyzed, the data would show no relationship with any PM, even though $PM_{2.5}$ showed some relationship with metals at the industrial site. This indicates the relationship between PM_x and water quality may not be generalizable, and PM or $PM_{2.5}$ concentration alone is insufficient to know what the concentration of water pollutants will be in AWH water if the location is moved. While some water quality parameters have strong correlation with PM, such as relationships between $PM_{2.5}$ and Al, Ca and Fe at the industrial site, other parameters may not be able to be easily correlated. This indicates that while there is some positive relationship between air quality and water quality, these interactions are highly variable by site and what air or water quality features are being measured, and generalized air quality measurements may not be able to predict generalized water quality measurements.

Continuing to investigate the variability of AWH water quality between sites will better determine the range of contaminants found in the water. Future research and new studies should evaluate airborne particulate matter at each individual site of analysis to better understand the mechanistic relationship between air quality and water quality. Knowing more on the influence of $PM_{2.5}$ on water quality and

connecting different sources of $PM_{2.5}$ to the variation in water quality of AWH will assist relief efforts in providing safe drinking water. As air quality continues to change, monitoring should continue as it can vary diurnally, seasonally and annually.

The U.S. EPA has reported on the variability of PM composition throughout the United States (EPA, 2023). In the southwestern United States, particularly in the region of this study, $PM_{2.5}$ has a high fraction of crustal and organic carbon components. Meanwhile, in the Midwest there is a larger fraction of nitrates, similar distribution of organic carbon, and much lower crustal content. PM composition is likely to have a strong influence on AWH water quality. Differences in PM composition across regions can mean different distributions and concentrations of crustal, organic and inorganic compounds in AWH waters. Future analyses should interrogate both PM concentration and its composition at different sites to gain better mechanistic understanding of the proportion of trace metals and other elements entering AWH water.

A deeper understanding of air quality interactions with AWH water quality is also necessitated by the scenarios in which AWH would be utilized, such as post-wildfire disaster relief. Further research into the impacts of wildfires and their associated higher PM_x concentrations and composition on AWH water quality will be beneficial to test the limits and water treatment needs of this technology.

6. Conclusions

This study finds that there are site differences in air quality measured as particulate matter, and corresponding differences in AWH water quality measured as conductivity, turbidity, TOC and trace metals. We hypothesized that the industrial site would yield higher concentrations of water quality contaminants compared to the urban site, and that air PM concentrations would positively correlate with water metal concentrations. The results partially supported the hypotheses. Air and water contamination was greater at the industrial site compared to the urban site. The industrial site had higher concentrations of both PM_{10} and $PM_{2.5}$ than the urban site ($p < 0.001$). There were also site differences for AWH water quality for Al ($p = 0.04$), Ca ($p < 0.001$), K ($p < 0.001$) and Mn ($p < 0.001$), where the industrial site had significantly higher concentrations of these metals. Water quality was a function of air quality, but for only some parameters. There was a positive relationship between $PM_{2.5}$ and some metals (Al ($p = 0.02$), Ca ($p = 0.009$), Fe ($p = 0.049$)) at the industrial site. Additionally, we observed a dilution effect between the volume of water collected and concentration of contaminants in water. When larger amounts of water were collected, concentrations of water quality constituents such as metals and turbidity were reduced to current acceptable levels according to the U.S. EPA.

CRediT authorship contribution statement

Matthew Russell: Writing – review & editing, Writing – original draft, Visualization, Supervision, Software, Project administration, Methodology, Investigation, Formal analysis, Data curation, Conceptualization. **Alex Webster:** Writing – review & editing, Validation, Software, Formal analysis, Conceptualization. **Carl Abadam:** Validation, Supervision, Project administration, Investigation, Data curation. **Katelin Fisher:** Writing – review & editing, Validation, Resources, Conceptualization. **Stephanie Campbell:** Investigation. **Carmen Atchley:** Investigation. **Kana Radius:** Investigation. **Paris Eisenman:** Investigation. **Ashley Apodaca-Sparks:** Investigation. **Astrid Gonzaga:** Investigation. **Rui Liu:** Validation, Resources. **Patrick Hudson:** Writing – review & editing, Validation, Software, Resources, Formal analysis, Conceptualization. **Anjali Mulchandani:** Writing – review & editing, Visualization, Supervision, Software, Resources, Project administration, Methodology, Funding acquisition, Conceptualization.

Declaration of competing interest

The authors declare the following financial interests/personal relationships which may be considered as potential competing interests:

Anjali Mulchandani and Matthew Russell report financial support was provided by New Mexico Water Resources Research Institute. Anjali Mulchandani reports financial support was provided by National Science Foundation. Anjali Mulchandani reports financial support was provided by PepsiCo Inc. Rui Liu reports financial support was provided by National Institutes of Health. If there are other authors, they declare that they have no known competing financial interests or personal relationships that could have appeared to influence the work reported in this paper.

Acknowledgements

This work was funded by National Science Foundation Award #1914490, PepsiCo, Inc., and the 2023 Student Water Research Grant Program of the New Mexico Water Resources Research Institute (NM WRRI) which was funded by the New Mexico State Legislature (NMWRRI-SG-FALL2023). This research was partially supported by the Center for Metals in Biology and Medicine (CMBM) under NIH grant P20 GM130422 and the NM-INSPIRES Center under NIH grant P30 ES032755 for metal concentration quantification using ICP-MS.

We gratefully acknowledge the City of Albuquerque Environmental Health Department Air Quality Program and their field technicians, Don Jaramillo and Chris Luna. Their invaluable daily support at the field sites enabled seamless water quality sampling and access to air quality monitoring data.

Supplementary materials

Supplementary material associated with this article can be found, in the online version, at doi:10.1016/j.watres.2025.124213.

Data availability

Data will be made available on request.

References

Alastuey, A., Querol, X., Plana, F., Viana, M., Ruiz, C.R., Campa, A.S.D.L., Rosa, J.D.L., Mantilla, E., Santos, S.G.D., 2006. Identification and chemical characterization of industrial particulate matter sources in Southwest Spain. J. Air Waste Manage. Assoc. 56 (7), 993–1006. https://doi.org/10.1080/10473289.2006.10464502.

AlorAir Solutions Inc, 2024. AlorAir LGR industrial commercial dehumidifier auto shut off with pump. Compact, APP Control, cETL Listed, Up to 180 PPD (Saturation), for Garages and Flood Restoration. https://www.alorair.com/product-details/alorair-storm-lgr-extreme-smart-app-control.

American Public Health Association, 2017. Baird, R., Eaton, A. D., Rice, E. W., Bridgewater, L., American Water Works Association, & Water Environment Federation. *Standard Methods for the Examination of Water and Wastewater* (23rd edition.). American Public Health Association; WorldCat.org.

Banholzer, S., Kossin, J., Donner, S., 2014. The impact of climate change on natural disasters. In: Singh, A., Zommers, Z. (Eds.), Reducing Disaster: Early Warning Systems for Climate Change. Springer, Netherlands, pp. 21–49. https://doi.org/10.1007/978-94-017-8598-3_2.

Chemical elements, Minerals, Rocks, 2024. Composition of the crust. https://www.sandatlas.org/composition-of-the-earths-crust/.

City of Albuquerque: Environmental Health Department. (2022). *City of Albuquerque 2022 Annual Network Plan*.

Cohen, M.A., Ryan, P.B., 1989. Observations less than the analytical limit of detection: a new approach. JAPCA 39 (3), 328–329. https://doi.org/10.1080/08940630.1989.10466534.

Crank, K., 2025. Microbial characterization of an evaporative cooling tower and atmospheric water generator in Las Vegas. NV [[Conference presentation]].

EPA. (2019). *Integrated science assessment for particulate matter*.

EPA. (2023). *Overview of particulate matter (PM) air quality in the United States*.

EPA. (2024a). *PM NAAQS overview*.

EPA. (2024b). *Technical Assistance Document for the reporting of daily Air Quality – the Air Quality Index (AQI)*.

Formenti, P., Elbert, W., Maenhaut, W., Haywood, J., Andreae, M.O., 2003. Chemical composition of mineral dust aerosol during the Saharan Dust Experiment (SHADE)

airborne campaign in the Cape Verde region, September 2000. J. Geophys. Res.: Atmos. 108 (D18). https://doi.org/10.1029/2002JD002648.
Gayoso, N., Moylan, E., Noha, W., Wang, J., Mulchandani, A., 2024. Techno-economic analysis of atmospheric water harvesting across climates. ACS ES&T Engineering 4 (7), 1769–1780. https://doi.org/10.1021/acsestengg.4c00098.
Hasheminassab, S., Daher, N., Saffari, A., Wang, D., Ostro, B.D., Sioutas, C., 2014. Spatial and temporal variability of sources of ambient fine particulate matter. Atmos. Chem. Phys. 14 (22), 12085–12097. https://doi.org/10.5194/acp-14-12085-2014.
Hosein, H.R., Mitchell, C.A., Bouhuys, A., 1977. Daily variation in air quality. Archives Environ. Health: Int. J. 32 (1), 14–21. https://doi.org/10.1080/00039896.1977.10667246.
Jahne, M., King, D., Kovalcik, K., Donohue, M., Pfaller, S., Helmick, K., Eades, G., Pait, M., Nye, M., Thimons, S., Garland, J., 2023. Water quality assessment of AC condensate for onsite collection and use. https://cfpub.epa.gov/si/si_public_record_report.cfm?Lab=CESER&dirEntryId=357248.
Jahne, M., Pfaller, S., King, D., Donohue, M., Brinkman, N., Keely, S., Davis, B., Garland, J., 2024. Microbial risk management for atmospheric condensate collections. https://cfpub.epa.gov/si/si_public_record_report.cfm?Lab=CESER&dirEntryId=360586.
Jahne, M., Pfaller, S., King, D., Garland, J., Impellitteri, C., 2018. Evaluation of Atmospheric Water Generation Technology: Microbial Water Quality. US Environmental Protection Agency, Washington, DC, USA.
Mulchandani, A., Edberg, J., Herckes, P., Westerhoff, P., 2022. Seasonal atmospheric water harvesting yield and water quality using electric-powered desiccant and compressor dehumidifiers. Sci. Total Environ. 825, 153966. https://doi.org/10.1016/j.scitotenv.2022.153966.
Mulchandani, A., Westerhoff, P., 2020. Geospatial climatic factors influence water production of solar desiccant driven atmospheric water capture devices. Environ. Sci. Technol. 54 (13), 8310–8322. https://doi.org/10.1021/acs.est.0c00534.
O'Brien, P.J., Siraki, A.G., Shangari, N., 2005. Aldehyde sources, metabolism, molecular toxicity mechanisms, and possible effects on Human health. Crit. Rev. Toxicol. 35 (7), 609–662. https://doi.org/10.1080/10408440591002183.
Piao, J., Nam, S.W., Kim, Y., Park, E., 2023. Enhancing groundwater management using aggregated-data analysis and segmented robust regression: a case study on spatiotemporal changes in water quality. Sci. Total Environ. 899, 165981. https://doi.org/10.1016/j.scitotenv.2023.165981.
Pinheiro, J., Bates, D., DebRoy, S., Sarkar, D., Core Team, R., 2023. *nlme: linear and nonlinear mixed effects models* (Version R package version 3.1-162) [Computer Software]. https://CRAN.R-project.org/package=nlme.
Ramsayer, K.D., 2021. *NASA data helps builds resilience as disasters grow more intense* [Gov]. https://www.nasa.gov/missions/aqua/nasa-data-helps-builds-resilience-as-disasters-grow-more-intense/.
Richardson, S.D., Postigo, C., 2012. Drinking water disinfection by-products. In: Barceló, D. (Ed.), Emerging Organic Contaminants and Human Health. Springer, Berlin Heidelberg, pp. 93–137. https://doi.org/10.1007/698_2011_125.
Robinne, F., Hallema, D.W., Bladon, K.D., Flannigan, M.D., Boisramé, G., Bréthaut, C.M., Doerr, S.H., Di Baldassarre, G., Gallagher, L.A., Hohner, A.K., Khan, S.J., Kinoshita, A.M., Mordecai, R., Nunes, J.P., Nyman, P., Santín, C., Sheridan, G., Stoof, C.R., Thompson, M.P., Wei, Y., 2021. Scientists' warning on extreme wildfire risks to water supply. Hydrol. Process 35 (5), e14086. https://doi.org/10.1002/hyp.14086.
Schneider, S.R., Abbatt, J.P.D., 2022. Wildfire atmospheric chemistry: climate and air quality impacts. Trends Chem. 4 (4), 255–257. https://doi.org/10.1016/j.trechm.2021.12.004.
Shiklomanov, I.A., 1991. The world's water resources. Proceed. Int. Symposium Commemorate 25, 93–126.
Upadhyay, N., Clements, A., Fraser, M., Herckes, P., 2011. Chemical speciation of $PM_{2.5}$ and PM_{10} in South Phoenix, AZ. J. Air Waste Manage. Assoc. 61 (3), 302–310. https://doi.org/10.3155/1047-3289.61.3.302.
US EPA, O., 2015a. *Environments and contaminants—Criteria air pollutants* [Overviews and Factsheets]. https://www.epa.gov/americaschildrenenvironment/environments-and-contaminants-criteria-air-pollutants.
US EPA, O., 2015b. *Drinking water regulations and contaminants* [Collections and Lists]. https://www.epa.gov/sdwa/drinking-water-regulations-and-contaminants.
Wang, S., Gallimore, P.J., Liu-Kang, C., Yeung, K., Campbell, S.J., Utinger, B., Liu, T., Peng, H., Kalberer, M., Chan, A.W.H., Abbatt, J.P.D., 2023. Dynamic wood smoke aerosol toxicity during oxidative atmospheric aging. Environ. Sci. Technol. 57 (3), 1246–1256. https://doi.org/10.1021/acs.est.2c05929.
Wickham, H., François, R., Henry, L., & Müller, K. (2023). *dplyr: a grammar of data manipulation* (Version R Package version 1.1.3) [Computer Software]. https://CRAN.R-project.org/package=dplyr.
Xia, Q., Li, R., Qiu, G.Y., Liu, A., Geng, S., 2015. Chemistry analysis for atmospheric water utilization as drinking water. J. Environ. Eng. 141 (2), 04014058. https://doi.org/10.1061/(ASCE)EE.1943-7870.0000884.
Zeng, C., Mojiri, A., Ananpattarachai, J., Farsad, A., Westerhoff, P., 2024. Sorption-based atmospheric water harvesting for continuous water production in the built environment: assessment of water yield and quality. Water Res. 265, 122227. https://doi.org/10.1016/j.watres.2024.122227.